Proc. Natl. Acad. Sci. USA
Vol. 89, pp. 613–617, January 1992
Biophysics

Femtosecond spectral evolution of the excited state of bacterial reaction centers at 10 K

(photosynthesis/charge separation/mutant)

MARTEN H. VOS[†‡], JEAN-CHRISTOPHE LAMBRY[†], STEVEN J. ROBLES[§], DOUGLAS C. YOUVAN[§], JACQUES BRETON[‡], AND JEAN-LOUIS MARTIN[†¶]

[†]Laboratoire d'Optique Appliquée, Institut National de la Santé et de la Recherche Médicale Unité 275, Ecole Polytechnique–Ecole Nationale Supérieure de Techniques Avancées, 91120 Palaiseau, France; [‡]Service de Biophysique, Département de Biologie, Centre d'Etudes Nucleaires de Saclay, 91191 Gif-sur-Yvette Cedex, France; and [§]Department of Chemistry, Massachusetts Institute of Technology, Cambridge, MA 02139

Communicated by Charles V. Shank, October 7, 1991

ABSTRACT **The femtosecond spectral evolution of reaction centers of *Rhodobacter sphaeroides* R-26 was studied at 10 K. Transient spectra in the near infrared region, obtained with 45-fs pulses (pump pulses centered at 870 nm and continuum probe pulses), were analyzed with associated kinetics at specific wavelengths. The t = 0-fs transient spectrum is very rich in structure; it contains separate induced bands at 807 and 796 nm and a bleaching near 760 nm, reflecting strong changes in interaction between all pigments upon formation of the excited state. A complex spectral evolution in the 800-nm region, most notably the bleaching of the 796-nm band, takes place within a few hundred femtosecond—i.e., on a time scale much faster than electron transfer from the primary donor P to the bacteriopheophytin acceptor H_L. The remarkable initial spectral features and their evolution are presumably related to the presence of H_L, as they were not observed in the D_{LL} mutant of *Rhodobacter capsulatus*, which lacks this pigment. A simple linear reaction scheme with an intermediate state cannot account for our data; the initial spectral evolution must reflect relaxation processes within the excited state. The importance for primary photochemistry of long distance interactions in the reaction center is discussed.**

The reaction center of photosynthetic purple bacteria contains an ensemble of six chromophores, which are bound to two protein subunits L and M (1, 2). Two of the chromophores are bacteriopheophytins (H_L and H_M); the other four are the bacteriochlorophylls P_L, P_M, B_L, and B_M. It is generally accepted that the former two are strongly coupled; they are referred to as the special pair P. Furthermore, not only P_L and P_M, but all chromophores display at least some degree of interaction. The ground state absorption spectrum in principle may consist of bands that each contain contributions of all six chromophores. The individual Q_Y bands are usually named after the chromophores that are thought to provide the major contribution—i.e., B (B_L and B_M), for *Rhodobacter sphaeroides* around 800 nm, and H (H_L and H_M) around 750 nm, and the exciton bands of P (P_- around 890 nm at cryogenic temperatures; P_+ around 810 nm). In addition to interchromophore interactions, the spectrum presumably is influenced by charge transfer transitions (3, 4) and by electrostatic interactions with the protein solvent (5–7). Various calculations of exciton interactions have been published, but the degree of excitonic coupling, the environmental influences, and the possible contribution of charge transfer transitions to the spectrum are still subject to debate (5–7). An alteration of the electronic state is bound to perturb any interaction and, viewing the reaction center as an interacting hexamer, modify all bands. For example, compared to that of the singlet ground state, the triplet spectrum displays considerable changes in the B bands and also minor perturbations of the H bands, apart from the very strong changes in the P bands (8). These features have been explained in terms of excitonic coupling (9).

The assessment of interpigment and pigment–protein interactions may prove essential to understand the nature of the extremely fast electron transport in the reaction center. Therefore, of high functional interest is the spectrum of the lowest singlet excited state of the reaction center pigment system P*, which is the precursor of electron transport. The kinetics of this state are most easily probed by its stimulated emission. In active *R. sphaeroides* reaction centers, it decays initially with a time constant of ≈3 ps at room temperature (10–12) and 1.2 ps at 10 K (13, 14). The charge pair $P^+H_L^-$ emerges with about the same time constant, as probed by the appearance of an electrochromic shift of the B band and the bleaching of the H_L band (10, 11, 13).

Recent data indicate that the spectrum of the reaction center also evolves on a time scale faster than the electron transfer from P to H_L. At room temperature, a kinetic component with a time constant of 0.9 ps was observed by Holzapfel *et al.* (12, 15). These data were interpreted in terms of a two-step sequential model, with the intermediate population of the state $P^+B_L^-$. Alternatively, the wavelength dependency of kinetics in the B-band region were interpreted in terms of intrinsic sample inhomogeneity by Kirmaier and Holten (16). Moreover, in our laboratory we have recently observed oscillatory features in the transient kinetics at cryogenic temperatures (17). These oscillations have periods of about 700 fs and 2 ps. The former are better observed in the absorption kinetics around 800 nm and the latter in the kinetics of stimulated emission. We have proposed that they reflect conservation of vibrational phase on the time scale of electron transport. The 2-ps mode might be directly coupled to electron transfer, but this has to be proved. Also, we observed a very fast kinetic component at 795 nm.

The observations of all groups may be related. It is now clear that spectral changes occur on a time scale shorter than $P^+H_L^-$ formation. To establish the spectrum of P* as it is initially formed and to study the origin of the fast spectral changes, we have collected transient femtosecond spectra in which the distortion due to dispersion effects is minimized in the Q_Y absorption region. The measurements were performed at 10 K to allow better spectral resolution. The difference spectra, which display changes in the entire Q_Y region, are analyzed together with kinetic data at key wavelengths.

MATERIALS AND METHODS

Preparation of reaction centers of *R. sphaeroides* strain R-26 (10) and of *Rhodobacter capsulatus* D_{LL} chromatophores

The publication costs of this article were defrayed in part by page charge payment. This article must therefore be hereby marked "*advertisement*" in accordance with 18 U.S.C. §1734 solely to indicate this fact.

¶To whom reprint requests should be addressed.

devoid of antenna pigments (18) was as described. The quinone acceptor Q_A in *R. sphaeroides* R-26 was reduced by addition of 50 mM dithiothreitol to ensure complete back reaction between the flashes (17). At room temperature, this treatment has a similar effect (slower overall kinetics) as reduction with sodium dithionite (19), but reduction with dithiothreitol was found to be much more stable. The samples were diluted in 60% (vol/vol) glycerol to an OD of 0.5 at 870 nm in a cuvette with an optical path of 1 mm and were cooled in the dark to 10 K in a convection cryostat.

Generation and amplification of the compressed broad-band (25 nm width around 870 nm; the spectrum was cut off below 850 nm) pump pulses of 45 fs full width at half maximum, with a repetition rate of 30 Hz, are described elsewhere (17). The chirp in the probe beam, ≈1 ps in the wavelength region of 750–850 nm, is compensated with two prisms to ±50 fs, such that the central wavelength part (≈800 nm) arrives first (t = 0 fs is defined at the maximum of the cross-correlation function between the 870-nm pump and the probe at 800 nm). The remaining chirp still is comparable to the pulse width and hence spectra at early times are still moderately distorted. In the 780- to 820-nm region, however, the chirp is only ±10 fs. Hence, in this region the spectrum is essentially chirp-free on the time scale of the pulse. The probe beam is split in a test and a reference beam, which both pass through the sample (except when recording ground-state spectra) and the monochromator. The absorption changes were detected with a pair of diodes for kinetic measurements and with an optical multichannel analyzer (Princeton Applied Research OMA III), with a spectral resolution of ≈1 nm, for spectral measurements. Unless otherwise indicated, the pump and probe beams were polarized in parallel. Typically, 10–20% of the centers were excited upon each flash. The kinetics were independent of flash energy in this excitation range.

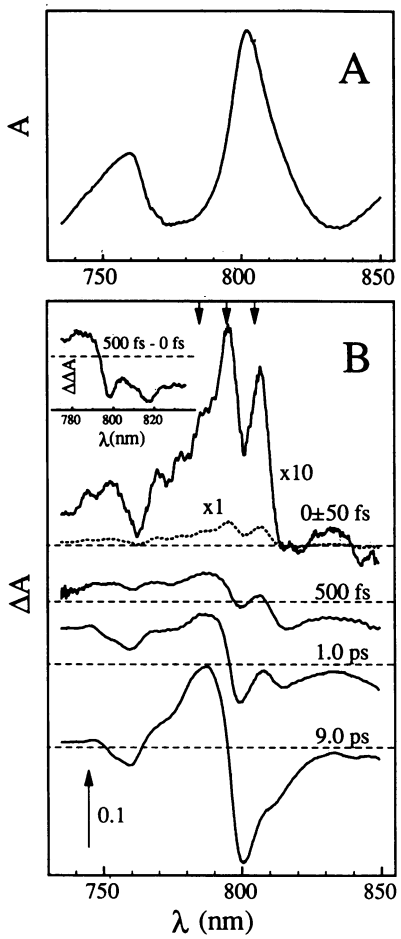

FIG. 1. Absorption (*A*) and transient absorption (*B*) spectra of reaction centers from *R. sphaeroides* R-26 obtained with the same apparatus. The chirp in the whole spectral range was ±50 fs. Arrows indicate wavelengths of the kinetics shown in Fig. 3 *B–D*. (*Inset*) Central part of the difference absorption spectrum obtained by subtracting the 0-fs from the 500-fs transient spectrum.

RESULTS

Spectra of *R. sphaeroides* R-26. The ground-state spectrum and the transient spectra of *R. sphaeroides* R-26 at different delay times are shown in Fig. 1. The spectrum taken at 0 ± 50 fs, that of the initially prepared excited state, is very rich in structure. It is dominated by two absorption bands, appearing in the B-band region of the ground-state spectrum, at 796 and 807 nm. In the H band, around 760 nm, a significant trough is observed in the broad absorption increase in this region. It should be noted that at 760 nm the t = 0-fs transient spectrum reflects less excited centers than at 800 nm due to the chirp of ≈30 fs between those wavelengths. Induced absorption is also observed in the region around 780 nm, where the ground state has little absorption. More to the red, a slight trough near 820 nm appears. This feature is assigned to the P_+ exciton band, which has its maximum around 810 nm (20) and here is partly masked by the rising 807-nm band.

The initial spectrum evolves to the well known (21) spectrum, which characterizes the state $P^+H_L^-$ and is dominated by an electrochromic blue shift of the B band (9-ps delay). However, several features in the evolution are remarkable. The induced absorption band around 807 nm remains present in the spectra at different delay times during the charge separation process. Presumably, it is a band associated with the disruption of the strong exciton coupling of P in the ground state. In contrast to the 807-nm band, the band that peaks at 796 nm very rapidly disappears. After 500 fs, when the electrochromic bandshift is only at ≈25% of its maximum amplitude, the feature is lost. Hence, the spectrum evolves on a time scale faster than that of the appearance of the electrochromic bandshift, which reflects $P^+H_L^-$ formation.

As explained in *Materials and Methods*, the complete (750–850 nm) t = 0-fs transient spectrum is still moderately distorted by the chirp effects and therefore direct quantitative comparison with the other transient spectra and with the

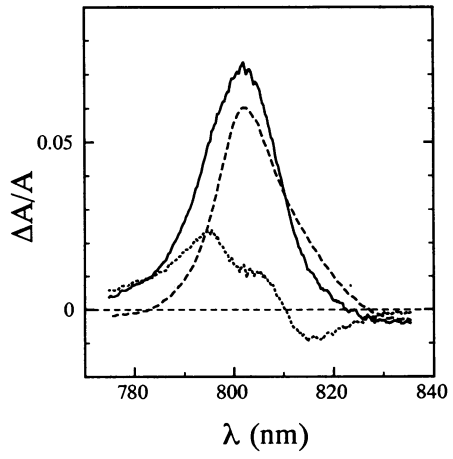

FIG. 2. Transient absorption (dotted line) at a polarization of 55° (magic angle) at t = 0 fs of reaction centers from *R. sphaeroides* R-26 in the B-band region. Ground-state absorption (dashed line) and t = 0-fs excited-state absorption spectrum (solid line), calculated by addition of the transient spectrum to the ground-state spectrum, normalizing for the percentage of excited centers.

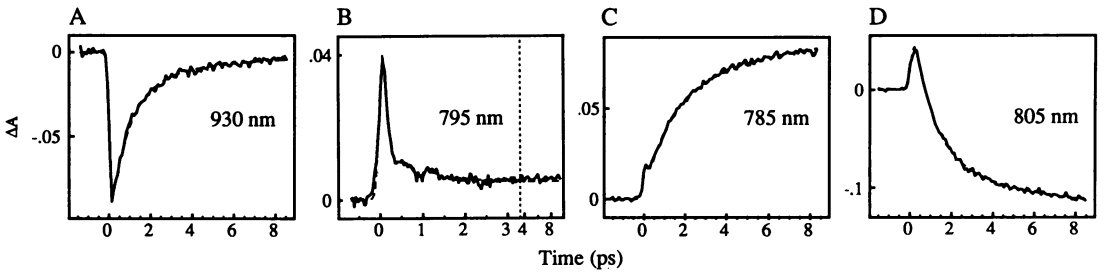

FIG. 3. Transient absorption kinetics of stimulated emission of reaction centers from *R. sphaeroides* R-26 at various wavelengths. Dashed lines are best fits to exponential decay functions (in *B* a damped cosine is superimposed). The fit parameters are listed in Table 1. Note the different time scale in *B*.

ground-state spectrum is not possible. However, Fig. 1 (*Inset*) highlights the spectral evolution in the 780- to 820-nm region, which is essentially free of chirp, between 0 and 500 fs. The relaxation of the induced 796-nm band is clearly seen superimposed on the appearing bandshift. Any other rapid spectral changes in the B-band region are masked by the band shift and need to be revealed by kinetic measurements.

To directly compare the transient and the ground-state spectrum at 0 fs (at 800 nm), we have collected a spectrum with the probe beam polarized at 55°, so that photoselection effects are canceled. This transient spectrum (Fig. 2) was then added to the ground-state spectrum (normalized for the percentage of excited centers probed) to obtain the absolute shape of the B-band absorption region of the initially formed excited state. Direct comparison shows that, apart from the apparent shift, the induced oscillator strength in the blue part of the B band is considerable, in the order of magnitude of the oscillator strength of the ground state.

Kinetics of *R. sphaeroides* R-26. The kinetics of the P* state of *R. sphaeroides* at 10 K, as monitored by the stimulated emission at 930 nm, are depicted in Fig. 3*A*. As with recently reported 100 K data (17), we are able to resolve that the kinetics are not single exponential; the data could be fitted significantly better with a double-exponential function [0.9 (80%) and 4.5 ps] than with a single-exponential function. In the data shown here, no oscillations can be resolved because of the short and spectrally broad pump pulses used (17).

The kinetics at 795 nm, near the peak of the bluemost band of the t = 0-fs transient spectrum (Fig. 1), are shown in Fig. 3*B*. The initially induced absorption relaxes very fast and the remaining signal decays within a few picoseconds. The signal is modulated by a damped oscillation. We fitted these data to the superposition of an exponentially damped cosine and a biexponential decay. When a time constant of 0.9 ps (derived from the stimulated emission) for the slower decay was imposed, a time constant of 90 fs was found for the fast decay; the period and damping time constant of the oscillation were found to be 0.65 ps [similar to that at 100 K (17)] and 0.8 ps, respectively. It should be stressed that no attempt was made to extract a rate constant and that this fit should be regarded as only indicative for the order of magnitude of the fast decay time, in view of (*i*) the extreme speed of the initial relaxation, (*ii*) the assumption of single exponential decay, which is not *a priori* justified, and (*iii*) the oscillatory modulation of the signal, which we described by a simple damped cosine. However, the initial evolution at this wavelength is not limited by the time resolution (≈25 fs).‖ The remaining overall kinetic evolution (the ≈0.9-ps component of the fit) may reflect slower phases of the initial relaxation and/or the electrochromic bandshift. The absorption does not decay on the time scale of a few picoseconds at 795 nm.

The kinetics at 785 and 805 nm are shown in Fig. 3 *C* and *D*, respectively. At these wavelengths, the kinetics are dominated by the strong bandshift and no oscillations with several periods could be resolved in the signals. The kinetics at 785 nm clearly display initial fast decay of an induced absorption. Hence, the fast spectral evolution extends to this wavelength region, where the ground state absorbs very little. This cannot be seen directly in the spectral evolution (Fig. 1), because of the dominating effect of the bandshift. The kinetics can be fitted with (fixed) time constants of 90 fs and 0.9 and 4.5 ps (Table 1). It should be noted that the amplitude ratio of the latter two components, which presumably reflect the bandshift, is 50:50—i.e., the kinetics are slower than those of the stimulated emission.

The kinetics at 805 nm, near the redmost peak of the t = 0-fs transient spectrum, do not visually show a fast transient, but part of the initial rise of the absorption increase is significantly slower than the instrumental response. This indicates that at this wavelength a fast kinetic component with a sign opposite that at 785 and 795 nm is present. Indeed, the kinetics can be fitted much better with three exponentials (90 fs and 0.9 and 4.5 ps) than with two exponentials (0.9 and 4.5 ps). The ratio of the 0.9- and 4.5-ps phases is 70:30 (Table 1) and hence the kinetics of the bandshift, as probed at this wavelength, are faster than those at 785 nm but still slightly slower than those of the stimulated emission.

Combining the spectral and kinetic data, it can be seen that the fast spectral evolution comprises a relaxation of (*i*) the narrow induced 796-nm band and (*ii*) the induced absorption shoulder near 785 nm as well as of an absorption increase in the 805-nm region. This concomitant spectral evolution on both sides of the induced absorption band may indicate that some of this band is redshifted during the relaxation. Substantial broadening of the 796-nm band can also not be excluded.

The initial relaxation is measured with very short optical pulses and partly in the regime of pump/probe temporal overlap. Therefore, we must consider the possibility that the spectral changes reflect interaction effects between the pump

Table 1. Amplitudes of absorption transients fitted to the function $A_1e^{-t/0.09} + A_2e^{-t/0.9} + A_3e^{-t/4.5} + A_4$ (t in ps and A in 10^{-3} OD)

	785 nm	795 nm†	805 nm	930 nm
A_1	52	79	−91	—
A_2	−41	7	148	−84
A_3	−48	—	65	−18
A_4	91	5	−122	−1

†A damped cosine (period, 0.65 ps; damping time, 0.8 ps) was superimposed on the decay in the fit.

‖In other recent work, which focused on the oscillatory features (17), we fitted kinetics at 100 K, 796 nm, with two exponentials, of which the fastest decayed with the instrumental response. The relatively strong presence of slower relaxation phases and oscillations (not included in the fit) under these conditions did not allow us to determine whether the fastest phase was significantly slower than the instrumental response.

and the probe rather than population processes induced by the pump pulse only (22). Two observations indicate that such pump/probe coherence effects are not the main cause of the present relaxation: (*i*) the relaxation is significantly slower than the decay of pump/probe overlap and (*ii*) the main spectral feature of the fast evolution is the relaxation of a band at 796 nm, outside the spectral range of the pump.

***R. capsulatus* D_{LL}.** An important question is whether the very fast (90 fs) spectral relaxation observed is related to electron transport. To investigate this point, we monitored the early transient spectra of the D_{LL} mutant of *R. capsulatus*, which lacks the bacteriopheophytin acceptor H_L and is incapable of electron transfer (18, 23). These spectra (not shown) consist of a bleaching near 815 nm, a single narrow induced band at 804 nm, and a broad induced absorption at the blue side of the spectrum; they do not display a relaxing band similar to the 796-nm band in *R. sphaeroides* R-26. Kinetics in the 795-nm region display a very small fast initial relaxation, which may well be due to part of the oscillations that also are seen in this wavelength region (17) or to a pump/probe coherence effect. Furthermore, apart from oscillatory features in the first few picoseconds, the spectral shape remains unchanged throughout the lifetime of P*, a few hundred picoseconds.

DISCUSSION

Our data constitute a dynamical spectral characterization at low temperature of the P* state of purple bacteria that perform the physiological charge separation reaction. They contain several remarkable features. In contrast to the transient spectra of *R. capsulatus* D_{LL}, the t = 0-fs spectrum of *R. sphaeroides* R-26 is surprisingly rich in structure. Moreover, the spectrum strongly evolves on a time scale on the order of 100 fs. These extremely fast spectral changes could not be resolved in an earlier study of *R. sphaeroides* at low temperature (13) because of the limited time resolution and signal/noise ratio.

The Nature of the t = 0-fs Transient Spectrum of *R. sphaeroides* R-26. The t = 0-fs transient spectrum is far too complicated to be described by the bleaching of a dimer ground state and the concomitant appearance of a broad absorption band, as it is often implicitly assumed, upon the formation of P*. It seems clear that at least four bands (at 807 nm, 796 nm, around 785 nm, and the broad feature on the blue side of the spectrum) and an additional trough (at 760 nm) appear. The appearing 807-nm band (and the 804-nm band in the D_{LL} mutant), which seems to persist as long as P is not in the singlet ground state (8, 20, 21), may be attributed to the disappearance of strong dimeric interactions in P. The strong remaining overall increase in oscillator strength in the B-band region indicates that these features are not (solely) due to small bandshifts. Several possibilities may be envisaged to explain the complexity of the t = 0-fs transient spectrum.

(*i*) The electronic coupling in the entire pigment system may be perturbed upon formation of the excited state, leading to bandshifts and changes in intensity borrowing between bands. A quantitative analysis of the essentially chirp-free part of the spectrum (not shown) indicated that the increase in oscillator strength in the B-band region amounts to >60% of the oscillator strength that can be attributed to the "monomeric" bacteriochlorophylls in the ground-state spectrum. Although it is difficult to make a clear distinction between bandshifts and net absorbance changes in the H-band region, the pronounced trough in the t = 0-fs transient spectrum of *R. sphaeroides* R-26 at 760 nm may indicate that at least part of this oscillator strength comes from the bacteriopheophytin, and in particular H_L, absorption region. This suggests that the perturbation of the interaction between the pigments not constituting P is significant. The more featureless transient spectrum of the D_{LL} mutant is consistent with the proposed role of H_L in the transient spectrum of *R. sphaeroides* R-26.

(*ii*) The transient spectrum is regarded as that of an isolated dimer. In this case, it must be assumed that there are many closely spaced higher electronic states (S_2, S_3, etc.) to which transition from the S_1 state may occur. We cannot exclude this possibility. However, it is unlikely in view of the facts that less features are observed in the Q_Y region of (*a*) the t = 0-fs transient spectrum of *R. capsulatus* D_{LL} and (*b*) the transient spectrum associated with the formation of the excited state in model porphyrin dimers (24).

(*iii*) Bandshifts may arise from altered electrostatic fields within the reaction center, due to formation of charge transfer states in P*. An intradimer charge transfer state would, in this view, lead to opposed shifts of B_L and B_M. This might explain the double-band structure of the t = 0-fs transient spectrum around 800 nm. However, these bands do not display the same fast relaxation, as would be expected, and also bandshifts cannot explain the net increase in oscillator strength in this region.

Altogether, it seems most likely that the highly structured transient spectrum of *R. sphaeroides* R-26 reflects changes in the excitonic interactions between all pigments upon formation of the excited state. If this is true, such interactions are considerable in at least either the ground state or the excited state and the pigment–protein complex may even be regarded as a rather strongly coupled hexamer in which the different absorption bands carry oscillator strength from, in principle, all pigments. Comparison of calculated and measured steady-state spectra have indicated that the six pigments in reaction centers of purple bacteria interact (3–6), and admixture of oscillator strength near 795 nm with P has been proposed on the basis of a photon echo excitation spectrum (25), but no consensus has been reached on the extent of these interactions and on the role of charge transfer states in these interactions. Our dynamic experiment suggests that interpigment interactions are observable; however, no calculations of the excited state spectrum are available for direct comparison with our data.

Spectral Evolution. The picture of spectral evolution that emerges from this study is clearly more complicated than that which could be extracted from early studies of our (10, 13, 19) and other (11, 26) groups. The spectral evolution of the stimulated emission (Fig. 3*A*) and of the slower phases in the absorption (Fig. 1, 500 fs to 9 ps) undoubtedly reflects oxidation of the primary donor, whatever the exact mechanism of this process, as extensively documented (11–14, 16, 19). The kinetics of the slower phases of the optical transients (including those of stimulated emission) are non-single exponential and wavelength dependent. These findings would be consistent with electron transport coupled to low frequency anharmonic vibrational motion, as explained elsewhere (27). However, other explanations, such as inherent reaction center inhomogeneity (16) cannot be excluded. Strongly nonexponential kinetics of the primary charge separation have also been reported for the green nonsulfur bacterium *Chloroflexus aurantiacus* (28, 29).

The complex spectral evolution on a very short time scale deserves more discussion. The fastest phases (≈90 fs) are clearly separated in time scale from the picosecond phases of charge separation, but the presence of intermediate phases cannot be excluded. Clearly, in view of the interference of coherent oscillations with the kinetics and the apparent multiplicity and wavelength dependence of the kinetic components, a discussion of the complex spectral evolution in terms of a strictly linear reaction scheme between distinct states, based on kinetics at single wavelengths, seems meaningless. The fits shown with the experimental data should therefore be regarded as indicative of the time scale of processes only.

However, it is illustrative to see what happens when we try to force the data into a linear two-step sequential model with the population of an intermediate electronic state, in spite of the above arguments. This scheme would be compatible with the kinetics of stimulated emission, which presumably reflect P* directly, only if the second step is the fastest step (cf. refs. 12 and 15). The very high ratio of the time constants of the two steps in our case (on the order of 10 if we take only the 0.9-ps phase of P* decay and even much higher for the slower phase) implies that only a very low population of the intermediate state can be built up. A simple calculation in terms of this scheme with the kinetic parameters in Table 1 [using only the faster (0.9 ps) phase for the decay of P* and taking into account the 10% excitation] would give differential extinctions of -4 (ΔA) at 785 nm and -7 at 795 nm for the intermediate state. These values are clearly unphysical, whatever the nature of the intermediate state, and consequently this scheme cannot account for our data.

Hence, we propose that the initial spectral evolution reflects fast relaxations within the excited state. Such relaxations may involve (*i*) vibrational relaxation of higher frequency modes, which act more locally (30) than the low frequency modes reflected in the absorption kinetics (17), (*ii*) protein rearrangements [molecular dynamics simulations have indicated that upon charge displacement within the reaction center the protein solvent relaxation takes place mainly by rearrangements of small dipolar sidegroups—i.e., by local movements—and is completed within ≈300 fs (31)], and (*iii*) electronic relaxation. The initially formed excited state may have a charge transfer character, as has been suggested on the basis of Stark spectroscopy data (32, 33) and simulations of ground-state spectra (3, 4). Such a state may be unstable on the time scale of electron transfer and relax into another state, possibly also with charge transfer character. Photon echo experiments indicate that an electronic relaxation process takes place within 100 fs (25). Although in most papers the intradimer charge transfer states $P_L^+P_M^-$ and $P_M^+P_L^-$ are considered as most important (4, 32–34) (but see ref. 3), the other pigments may be involved to a lesser extent. The possible importance of charge transfer states for electron transport has been pointed out by several authors (3, 34–36). An interpigment charge displacement immediately after excitation is consistent with our previous proposal (17) that electron transfer may be coupled to collective protein vibrational modes. The subsequent relaxation may then be part of coherent electron transfer toward H_L.

Upon formation of the excited state, oscillations are coherently activated, which must represent collective motion of the pigment–protein complex in view of their low (≈15 cm^{-1}) frequency values (17). The expression of these oscillations in the optical transients demonstrates efficient electron–phonon coupling. The transient spectrum of the initially prepared excited state seems to involve most, if not all, pigments, including H_L. The delocalized character of this initial excited state is consistent with the efficient coupling to collective vibrational modes. The experiments with the *R. capsulatus* D_{LL} mutant indicate that key features of the initial transient spectrum and the subsequent fast spectral evolution are related to the presence of H_L in the reaction center. An interesting finding in this context is that the vector of the electron transport process responsible for the depletion of P* seems to be directed directly to H_L (34, 37). Primary electron transport seems to involve direct coupling between distant parts of the reaction center complex.

Part of this work has been supported by grants from the Institut National de la Santé et de la Recherche Médicale and Ecole Nationale Supérieure de Techniques Avancées (J.-L.M.) and from the Human Frontier Science Organization (J.B. and D.C.Y.). D.C.Y. was supported by Department of Energy Grant DE/FG02/90ER20019 and National Institutes of Health Grant R1GM42645A. M.H.V. is recipient of a grant from the Science Program of the European Economic Community.

1. Deisenhofer, J. P., Epp, O., Miki, K., Huber, R. & Michel, H. (1984) *J. Mol. Biol.* **180**, 385–398.
2. Allen, J. P. & Feher, G. (1984) *Proc. Natl. Acad. Sci. USA* **81**, 4795–4799.
3. Scherer, P. O. J. & Fischer, S. F. (1987) *Chem. Phys. Lett.* **141**, 179–185.
4. Parson, W. W. & Warshel, A. (1987) *J. Am. Chem. Soc.* **20**, 6152–6163.
5. Pearlstein, R. M. (1987) in *Photosynthesis*, ed. Amesz, J. (Elsevier, Amsterdam), pp. 299–317.
6. Hanson, L. K. (1988) *Photochem. Photobiol.* **47**, 903–921.
7. Friesner, R. A. & Won, Y. (1989) *Biochim. Biophys. Acta* **977**, 99–122.
8. Den Blanken, H. J. & Hoff, A. J. (1982) *Biochim. Biophys. Acta* **681**, 365–374.
9. Lous, E. J. & Hoff, A. J. (1987) *Proc. Natl. Acad. Sci. USA* **84**, 6147–6151.
10. Martin, J.-L., Breton, J., Hoff, A. J., Migus, A. & Antonetti, A. (1986) *Proc. Natl. Acad. Sci. USA* **83**, 957–961.
11. Woodbury, N. W., Becker, M., Middendorf, D. & Parson, W. W. (1985) *Biochemistry* **24**, 7516–7521.
12. Holzapfel, W., Finkele, U., Kaiser, W., Oesterhelt, D., Scheer, H., Stilz, H. U. & Zinth, W. (1990) *Proc. Natl. Acad. Sci. USA* **87**, 5168–5172.
13. Breton, J., Martin, J.-L., Fleming, G. R. & Lambry, J.-C. (1988) *Biochemistry* **27**, 8267–8284.
14. Fleming, G. R., Martin, J.-L. & Breton, J. (1988) *Nature (London)* **333**, 190–192.
15. Holzapfel, W., Finkele, U., Kaiser, W., Oesterhelt, D., Scheer, H., Stilz, H. U. & Zinth, W. (1989) *Chem. Phys. Lett.* **160**, 1–7.
16. Kirmaier, C. & Holten, D. (1990) *Proc. Natl. Acad. Sci. USA* **87**, 3552–3556.
17. Vos, M. H., Lambry, J.-C., Robles, S. J., Youvan, D. G., Breton, J. & Martin, J.-L. (1991) *Proc. Natl. Acad. Sci. USA* **88**, 8885–8889.
18. Robles, S. J., Breton, J. & Youvan, D. C. (1990) in *Reaction Centers of Photosynthetic Bacteria*, ed. Michel-Beyerle, M.-E. (Springer, Berlin), pp. 283–291.
19. Breton, J., Martin, J.-L., Petrich, J., Migus, A. & Antonetti, A. (1986) *FEBS Lett.* **209**, 37–43.
20. Breton, J. (1988) in *The Photosynthetic Bacterial Reaction Center, Structure and Function*, eds. Breton, J. & Verméglio, A. (Plenum, New York), pp. 59–69.
21. Kirmaier, C., Holten, D. & Parson, W. W. (1985) *Biochim. Biophys. Acta* **810**, 49–61.
22. Brito Cruz, C. H., Gordon, J. P., Becker, P. C., Fork, R. L. & Shank, C. V. (1988) *IEEE J. Quantum Electron.* **24**, 261–266.
23. Robles, S. J., Breton, J. & Youvan, D. C. (1990) *Science* **248**, 1402–1405.
24. Bilsel, O., Rodriguez, J. & Holten, D. (1990) *J. Phys. Chem.* **94**, 3508–3512.
25. Meech, S. R., Hoff, A. J. & Wiersma, D. A. (1986) *Proc. Natl. Acad. Sci. USA* **83**, 9464–9468.
26. Kirmaier, C. & Holten, D. (1988) *FEBS Lett.* **239**, 211–218.
27. Martin, J.-L. & Vos, M. H. (1992) *Annu. Rev. Biophys. Biomol. Struct.*, in press.
28. Martin, J.-L., Lambry, J.-C., Ashokkumar, M., Michel-Beyerle, M. E., Feick, R. & Breton, J. (1990) in *Ultrafast Phenomena VII*, eds. Harris, C. B., Ippen, E. B., Mourou, G. A. & Zewail, A. H. (Springer, Berlin), pp. 514–528.
29. Becker, M., Middendorf, V., Nagarajan, V., Parson, W. W., Martin, J. E. & Blankenship, R. E. (1991) *Biochim. Biophys. Acta* **1057**, 299–312.
30. Gō, N., Noguti, T. & Nishikawa, T. (1983) *Proc. Natl. Acad. Sci. USA* **80**, 3696–3700.
31. Treutlein, H., Schulten, K., Niedermeier, C., Deisenhofer, J., Michel, H. & DeVault, D. (1988) in *The Photosynthetic Bacterial Reaction Center, Structure and Function*, eds. Breton, J. & Verméglio, A. (Plenum, New York), pp. 369–377.
32. Lösche, M., Feher, G. & Okamura, M. Y. (1987) *Proc. Natl. Acad. Sci. USA* **84**, 7537–7541.
33. Lockhart, D. J. & Boxer, S. G. (1987) *Biochemistry* **26**, 664–668, and correction (1987) *Biochemistry* **26**, 2958.
34. Boxer, S. G. (1990) *Annu. Rev. Biophys. Biophys. Chem.* **19**, 267–299.
35. Won, Y. & Friesner, R. A. (1988) *Biochim. Biophys. Acta* **935**, 9–18.
36. Warshel, A. (1980) *Proc. Natl. Acad. Sci. USA* **77**, 3105–3109.
37. Lockhart, D. J., Goldstein, R. F. & Boxer, S. G. (1988) *J. Chem. Phys.* **89**, 1408–1415.